Journal of Alloys and Compounds 522 (2012) 46–50

Contents lists available at SciVerse ScienceDirect

Journal of Alloys and Compounds

journal homepage: www.elsevier.com/locate/jallcom

Effects of nitrogen concentration on N-doped anatase TiO_2: Density functional theory and Hubbard *U* analysis

Hsuan-Chung Wu [a,b,*], Syuan-Wei Lin [a], Jhao-Sian Wu [a]

[a] Department of Materials Engineering, Ming Chi University of Technology, New Taipei 24301, Taiwan
[b] Center for Thin Film Technologies and Applications, Ming Chi University of Technology, New Taipei 24301, Taiwan

ARTICLE INFO

Article history:
Received 5 October 2011
Received in revised form 6 January 2012
Accepted 15 January 2012
Available online 2 February 2012

Keywords:
N-doped TiO_2
First principles
Photocatalyst
Electronic structure

ABSTRACT

To fully comprehend the photocatalytic mechanisms of anatase $TiO_{2-x}N_x$ of various nitrogen concentrations, this study performed first principles calculations based on density functional theory, employing Hubbard *U* on-site correction, to evaluate the crystal structure, impurity formation energy, and electronic structure. An effective Hubbard *U* of 8.47 eV was adopted to correctly determine the band gap of pure anatase TiO_2. The calculations show that increasing the concentration of nitrogen requires greater formation energy during the synthesis of N-doped TiO_2. Under light nitrogen doping ($\leq$6.25 at.%), N isolated impurity states form above the top of valence band meanwhile the band gap does not change noticeably. Under heavy nitrogen doping ($\geq$8.33 at.%), a narrowing of the band gap and broadening of the valence band occur, which might explain the red shift at the edge of the optical absorption range observed in some experimental studies. These findings provide a reasonable explanation of recent experimental results.

1. Introduction

Reducing environmental pollution and developing renewable energy sources are two issues of global concern. Titanium dioxide (TiO_2) has attracted considerable attention in the degradation of environmental pollutants and the conversion of solar energy due to its high photocatalytic activity, nontoxicity, low cost, and chemical stability. However, anatase TiO_2 only absorbs ultraviolet (UV) light (less than 387 nm) due to its wide band gap (3.2 eV). UV light accounts for a small fraction (~5%) of solar energy and therefore its solar energy utilization is very low. Limitations due to the wide band gap make TiO_2 ineffective for many potential applications. Because visible light (400–700 nm) accounts for a large fraction (~45%), extending optical absorption to the visible light region in wide band gap semiconducting materials has become a well researched topic in recent years.

A great deal of research has gone into modifying the band gap of TiO_2, using a variety of approaches [1]. One of the most effective methods has been doping the TiO_2 with impurity elements including transition metals, noble metals, and nonmetals. Since Asahi et al. [2] reported in 2001 that doping with nitrogen can enhance photocatalytic activity under visible light irradiation, TiO_2 has been doped with a variety of nonmetal elements, such as N [3–8], S [9], B [10], F [11], C [12] and P [13] to study its photocatalytic activity under visible light, with nitrogen doping proving to be particularly effective. Asahi et al. [2] indicated that the N 2p states could hybridize with O 2p states, resulting in a narrowing of the band gap with the material becoming photoactive in the visible light region. However, other studies supported the notion that N-doping does not cause a narrowing of the band gap of TiO_2 [3,4]. For example, Irie et al. [4] prepared $TiO_{2-x}N_x$ ($x < 0.02$) powders and formed an isolated narrow band above the valence band. It was determined that the isolated N 2p band was responsible for the response to visible light. On the theoretical side, Yang et al. [5] investigated the effects of nitrogen concentration (0–4.17 at.%) on electronic band structure using calculations based on density functional theory (DFT). The calculated band gap of pure anatase was approximately 2.2 eV, which represents an underestimation of approximately 30% compared with the experimental value of 3.2 eV. Underestimations always result from band gap calculations due to well-known limitations related to DFT theory. The results show that at reduced doping levels, a number of localized N 2p states formed above the valence band in N-doped anatase, leading to a reduction in the photon transition energy. As the doping level was increased, the energy gap narrowed only slightly compared with lower doping levels. Recently, doping with high concentrations of nitrogen has been achieved using novel processes, which have resulted in a significant reduction in the band gap. Wu et al. [6] synthesized $TiO_{2-x}N_x$ thin films using ion-beam-assisted deposition to obtain a wide range of nitrogen concentrations. The results show a decreasing trend in the

* Corresponding author at: Department of Materials Engineering, Ming Chi University of Technology, 84 Gungjuan Road, Taishan, New Taipei 24301, Taiwan. Tel.: +886 2 29089899x4675; fax: +886 2 29084091.
E-mail address: hcwu@mail.mcut.edu.tw (H.-C. Wu).

0925-8388/$ – see front matter © 2012 Elsevier B.V. All rights reserved.
doi:10.1016/j.jallcom.2012.01.071

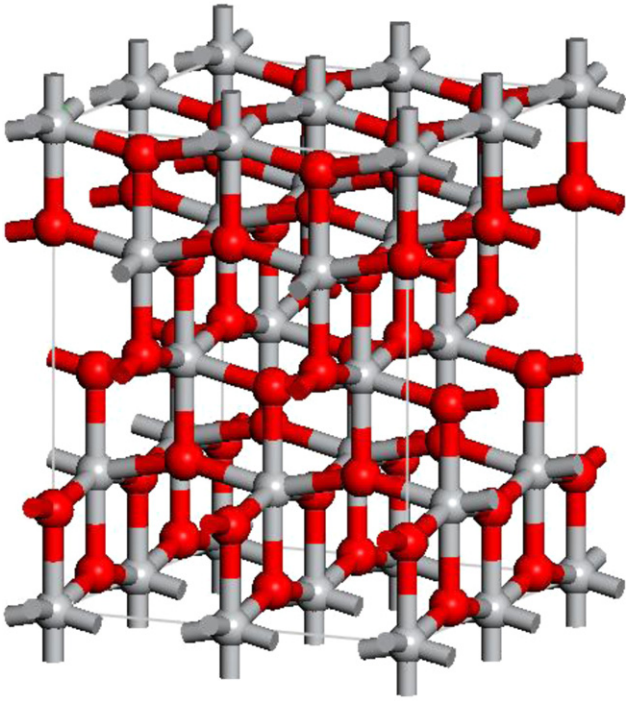

Fig. 1. The $2 \times 2 \times 1$ supercell model considered in this work. Red and gray spheres represent O and Ti atoms, respectively. (For interpretation of the references to color in this figure legend, the reader is referred to the web version of the article.)

band gap of the films within a particular range of increasing dopant concentrations, with the minimum band gap of 2.67 eV, occurring at $x = 0.71$ (23 at.%). In 2011, Jiang et al. [7] introduced a novel process combining the technique of plasma nitriding and micro-arc oxidation to prepare high concentration N-doped TiO_2 film ($TiO_{2-x}N_x$, x to 0.11), exhibiting a significant red-shift in the band gap transition, a narrow band gap of 2.6 eV, higher photo-generated charge carrier density, and improved photocatalytic properties.

As discussed above, the origin of the visible light photoactivity of N-doped TiO_2 remains an issue of debate. In addition, most theoretical calculations greatly underestimate the band gap in TiO_2 due to the adoption of conventional DFT method, which is known to include an insufficient description of the on-site Coulomb interaction between electrons occupying the Ti 3d orbitals. In this paper, first principles calculations employing the DFT + U (Hubbard U) approach are performed to investigate the crystal structure, formation energy, electronic structure, and charge density of N-doped anatase $Ti_xO_{2-x}N_x$. Various concentrations of nitrogen, $x = 0.0625$, 0.125, 0.1875, 0.25 and 0.3125 (2.08, 4.17 and 6.25, 8.33 and 10.42 at.%), are analyzed.

2. Calculation models and methods

Anatase TiO_2 has a tetragonal structure belonging to the spatial group I41/AMD with lattice parameters $a = b = 3.776$ Å, $c = 9.486$ Å. Doping systems were constructed from a 48-atom anatase supercell with a $2 \times 2 \times 1$ repetition, as shown in Fig. 1. The N-doped configuration was constructed by replacing one oxygen atom with one nitrogen atom. The reason to choose substitutional N-doped TiO_2 was that the substitutional model required much smaller formation energy than the interstitial doping model. Different substitutional nitrogen doping levels were modeled by substituting one, two, three, four, or five oxygen atoms in the 48-atom supercell. The x values of the $TiO_{2-x}N_x$ system were $x = 0.0625$, 0.125, 0.1875, 0.25 and 0.3125, which correspond to 2.08, 4.17, 6.25, 8.33 and 10.42 at.%, respectively.

First principles calculations were performed using the CASTEP module [14] in Materials Studio 5.0 developed by Accelrys Software Inc. Electron-ion interactions were modeled using ultrasoft pseudopotentials in the Vanderbilt form [15]. The valence atomic configurations were $2s^22p^4$ for O, $2s^22p^3$ for N and $3s^23p^63d^24s^2$ for Ti. The wave functions of the valence electrons were expanded through a plane wave basis set and the cutoff energy was selected as 400 eV. The Monkhorst–Pack scheme [16] K-points grid sampling was set at $4 \times 4 \times 3$ (less than 0.04 $Å^{-1}$) in the supercells. The convergence threshold for self-consistent iterations was set at 5×10^{-6} eV. In the optimization process, the energy change, maximum force, maximum stress, and maximum displacement tolerances were set at 9×10^{-5} eV/atom, 0.09 eV/Å, 0.09 GPa, and 0.009 Å, respectively. To more accurately describe the electronic structures, the DFT + U method was adopted and the strong on-site Coulomb repulsion among the localized Ti 3d electrons was described using the following formalism [17,18]:

$$E_{\mathrm{DFT+U}} = E_{\mathrm{DFT}} + \frac{U-J}{2}\Sigma_\sigma Tr[\rho^\sigma - \rho^\sigma\rho^\sigma] \quad (1)$$

where ρ^σ denotes the spin (σ) polarized on-site density matrix. The spherically averaged Hubbard parameter U describes the increase in energy caused by placing an extra electron at a particular site, and the parameter J (1 eV) represents the screened exchange energy. The effective Hubbard parameter $U_{\mathrm{eff}} = U - J$, which accounts for the on-site Coulomb repulsion for each affected orbital, is the only external parameter required in this approach.

3. Results and discussion

3.1. Structural optimization

The lattice parameters, average bond lengths and volume ratio of the optimized supercell, obtained from geometric optimization, are summarized in Table 1. The optimized crystal parameters of pure TiO_2 are $a = b = 3.778$ Å and $c = 9.549$ Å, which are in good agreement with the experimental values of $a = b = 3.782$ Å, $c = 9.502$ Å [19]. This result implies that our calculation methods are reasonable and the calculation results reliable. In anatase TiO_2, each Ti atom is bonded to its four nearest and two second nearest oxygen neighbors. Average bond lengths are represented as Ti—O^{1st} and Ti—O^{2nd}, respectively. For pure anatase TiO_2, the average Ti—O^{1st} and Ti—O^{2nd} are 1.931 and 1.986 Å, respectively. The Ti—O bond lengths in the N-doped structure are much longer than those of the pure TiO_2 and with a tendency to increase with increasing nitrogen concentration, as do the Ti—N bond lengths. At the same nitrogen concentration, most of the Ti—N bond lengths are longer than those of Ti—O. Therefore, the volume ratio of N-doped TiO_2 (V_N) to pure TiO_2 (V_p) also tends to increase with an increase in nitrogen concentration. This indicates that nitrogen doping causes an expansion of the cell volume for which there are two reasons. First, the radii of the ions differ: 1.71 Å for N^{3-} ions and 1.32 Å for O^{2-} ions. Second, compared with the O atom, the smaller electronegativity of the N atom induces a weaker attraction in the Ti—N bond and a longer bond length.

3.2. Hubbard U parameter

The DFT + U approach introduces an intra-atomic electron–electron interaction as an on-site correction in order to describe systems with localized d and f electrons, capable of producing an accurate band gap. Determination of an appropriate effective Hubbard U_{eff} parameter is necessary in DFT + U calculations to correctly interpret the intra-atomic electron correlation. As shown in Fig. 2, for anatase TiO_2 phases, the band gap widens when the effective Hubbard U_{eff} is increased. The band gap of anatase

Table 1
Optimized lattice parameters, average bond lengths and volume ratio of $TiO_{2-x}N_x$.

$TiO_{2-x}N_x$	Lattice parameters (Å)			Bond lengths (Å)				Volume ratio
x	a	b	c	Ti—O^{1st}	Ti—O^{2nd}	Ti—N^{1st}	Ti—N^{2nd}	V_N/V_p
0.0000	3.778	3.778	9.549	1.931	1.986			1.0000
0.0625	3.773	3.793	9.561	1.933	1.990	1.936	2.023	1.0038
0.1250	3.815	3.772	9.510	1.935	1.995	1.921	2.061	1.0037
0.1875	3.769	3.826	9.516	1.936	1.999	1.943	2.026	1.0067
0.2500	3.802	3.802	9.496	1.935	2.002	1.949	2.057	1.0071
0.3125	3.812	3.798	9.612	1.949	1.988	2.034	2.261	1.0215

can be effectively widened by increasing U_{eff} from 2 to 8 eV. Here, the effective on-site Coulomb interaction is U_{eff} = 8.47 eV for Ti 3d in the DFT + U approach, and the calculated band gap of pure anatase is 3.21 eV, which is very close to the experimental value.

3.3. Formation energy

To examine the relative stability of N-doped TiO_2 for different N concentrations, the defect formation energies were calculated according to the following formula:

$$E_f = E_{tot}(\text{N-doped}) - E_{tot}(\text{pure}) - n\mu_N + n\mu_O \quad (2)$$

Here, E_{tot}(N-doped) and E_{tot}(pure) are the total energies of N-doped TiO_2 and pure TiO_2, respectively; n is the number of substitutional nitrogen atoms; and μ_N and μ_O represent the chemical potentials of the N and O atoms, respectively. The formation energy depends on growth conditions, which can be Ti-rich or O-rich. For TiO_2, μ_{Ti} and μ_O satisfy the relationship $\mu_{Ti} + 2\mu_O = \mu_{TiO_2}$. Under the O-rich growth condition, μ_O is determined by the total energy of an O_2 molecule ($\mu_O = \mu_{O_2}/2$) and μ_{Ti} is determined by the formula $\mu_{Ti} = \mu_{TiO_2} - 2\mu_O$. Under the Ti-rich growth condition, μ_{Ti} is the energy of one Ti atom in bulk Ti and μ_O is determined by $\mu_O = (\mu_{TiO_2} - \mu_{Ti})/2$. The calculated formation energies for different N doping levels in TiO_2 are summarized in Table 2. It should be noted that the smaller the E_f value is, the easier it is to incorporate impurity atoms into the TiO_2 supercell. The formation energies associated with N-doped TiO_2 are reduced under Ti-rich conditions than under the O-rich conditions, indicating that the incorporation of N into TiO_2 at the O atom site is favorable. This makes it easier to incorporate N into the O matrix. In addition, the formation energies increase with an increase in N concentration under both Ti-rich and O-rich conditions, suggesting that the synthesis of the N-doped anatase TiO_2 system at a higher doping level becomes relatively difficult.

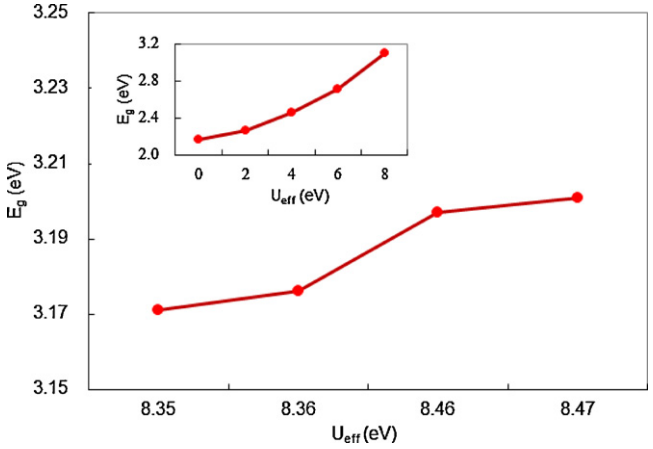

Fig. 2. Relationship between the effective Hubbard parameter (U_{eff}) and the band gap (E_g) of anatase TiO_2.

Table 2
Formation energy and average Mulliken population of $TiO_{2-x}N_x$.

$TiO_{2-x}N_x$	Formation energy		Mulliken population (|e|)		
x	Ti-rich	O-rich	Ti	O	N
0			1.470	−0.730	
0.0625	0.48	5.07	1.464	−0.737	−0.620
0.1250	0.96	10.15	1.454	−0.733	−0.610
0.1875	1.34	15.12	1.448	−0.733	−0.620
0.2500	2.22	20.59	1.443	−0.732	−0.623
0.3125	−0.80	22.17	1.276	−0.661	−0.522

3.4. Band structure

The calculated band structure for pure TiO_2 is shown in Fig. 3. The zero-point energy is taken as the Fermi level. The valence band maximum (VBM) and the conduction band minimum (CBM) are both located at the G point, indicating that pure TiO_2 is a direct-gap semiconductor material. The minimum gap between VBM and CBM (E_g) is 3.21 eV, which is consistent with the experimental value of 3.2 eV.

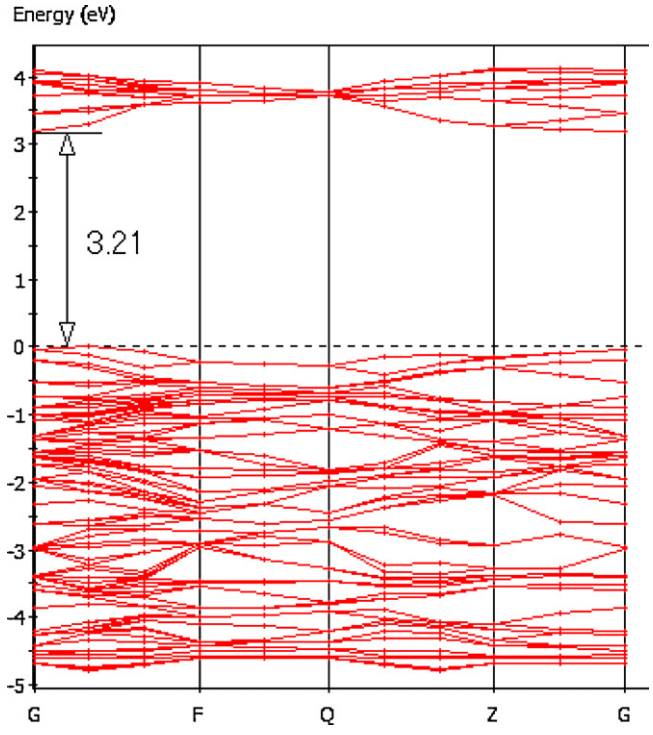

Fig. 3. Band structure for the 2 × 2 × 1 supercell of pure anatase TiO_2.

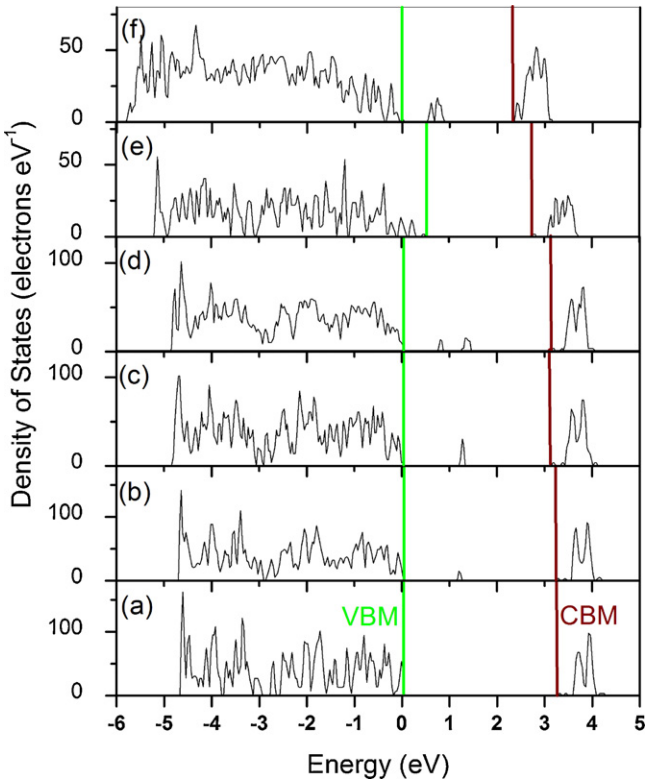

Fig. 4. Total density of states (TDOS) of $TiO_{2-x}N_x$ with (a) $x=0$, (b) $x=0.0625$, (c) $x=0.125$, (d) $x=0.1875$, (e) $x=0.25$ and (f) $x=0.3125$.

3.5. Density of states

To investigate the electronic properties of N-doped anatase TiO_2, the total density of states (TDOS) of each $TiO_{2-x}N_x$ system was calculated and is shown in Fig. 4. Other related values that were calculated include VBM, CBM, the width of the valence band, and the band gap, which are shown in Fig. 5(a)–(d) show that at lower concentrations, N doping in TiO_2 does not result in significant variations in VBM or CBM compared to pure anatase TiO_2. This implies that light nitrogen doping ($x \leq 0.1875$) does not noticeably influence the band gap of TiO_2. With an increase in the N doping levels, the CBMs at $x=0.25$ and $x=0.3125$ decrease to 2.79 and 2.36 eV, respectively (see Fig. 5(e)–(f)). Meanwhile, the VBM

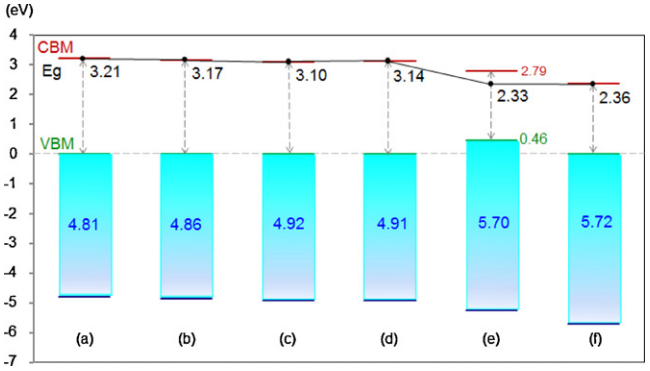

Fig. 5. The schematic illustrations of the band structure and calculated band energy position of $TiO_{2-x}N_x$ with (a) $x=0$, (b) $x=0.0625$, (c) $x=0.125$, (d) $x=0.1875$, (e) $x=0.25$ and (f) $x=0.3125$.

value increases to 0.46 at $x=0.25$ before subsequently decreasing to zero at $x=0.3125$. The band gaps at $x=0.25$ and $x=0.3125$ are 2.33 and 2.36 eV, respectively. Therefore, it should be emphasized that a narrowing of the band gap of N-doped TiO_2 occurs only for heavy nitrogen doping ($x \geq 0.25$). The narrowing of the band gap due to heavy nitrogen doping is the result of a decrease in CBM and an increase in VBM. The observed relationship between band gap and N concentration is similar to that described by Zhao's theoretical calculations [20]. As a result, the electron transition energy from the valence band to the conduction band decreased by approximately 0.88 eV as a result of heavy nitrogen doping, and thus may induce a red shift at the edge of the optical absorption range. In addition, it was found that the valence band broadens after N is incorporated into TiO_2, especially in the case of heavy nitrogen doping, which increases the mobility of the photo-generated electron–hole pair. Therefore, both the narrowing of the band gap and the increased mobility of photo-generated carriers in heavy nitrogen doping concentrations can improve the photocatalytic activity under visible light, as illustrated in recent experimental results [6,7].

To further analyze the constitution of each of the related orbitals in the TDOS, a projected density of states (PDOS) analysis of each configuration was performed, and the results are shown in Fig. 6. In pure anatase TiO_2 (Fig. 6a), the valence band mainly comprises O 2p states with a small number of Ti 3d states while the conduction band consists of Ti 3d states with a small number of O 2p states. This indicates that there exists a little covalence bond character between Ti and O atoms. The valence band of TiO_2 has a large bandwidth of approximately 5 eV, showing a strong delocalization among the O 2p electrons. At $x=0.0625$, it is clear from Fig. 6(b) that one isolated N 2p state is localized only 1.1 eV above the top of the VB of the host TiO_2, which is consistent with the calculations of Long and Ma [21,22]. This is because the N atom can receive two electrons and its 2p states are not fully occupied, leading to a shallow acceptor state localized only above the valence band. The electron in the VB can be excited to localized impurity states in the band gap and subsequently to the CB through absorption of visible light. However, empty N 2p states can act as traps for excited electrons, promoting electron–hole pair recombination. At $x=0.125$ and $x=0.1875$ (Fig. 6(c) and (d)), the isolated N 2p states are localized above the top of the VB, and are similar to the PDOS at $x=0.0625$. At $x=0.25$ (Fig. 6(e)), the strong hybridization of N and its first neighboring O atoms leads to an increase in VBM. The full overlap of the impurity band and valence band can reduce the number of charge carrier traps and suppress the recombination of photo-excited carriers. From $x=0.25$ to $x=0.3125$, the conduction band moves continuously toward the Fermi energy, resulting in a reduction of the band gap. This is due to the transformation of Ti^{4+} to Ti^{3+}. It has been proven that the reduction of Ti^{4+} to Ti^{3+} occurs in N-doped TiO_2 due to a charge imbalance between the O^{2-} and N^{3-} ions [23]. We discuss charge transformation in the following section.

3.6. Electronic density

Mulliken populations of each model are summarized in Table 2. At $x=0.0625$, the Mulliken population of N (-0.62 |e|) is larger than that of O (-0.737 |e|). This is because the electronegativity of N is lower than that of O. With an increase in the N concentration to $x=0.25$, variation in the charge of O and N is not obvious by, but the charge of the Ti atom decreases slightly. These results indicate that the incorporation of N results in ever fewer electrons transferring from Ti to O or N atoms. At $x=0.3125$, the Mulliken population of Ti atoms significantly decreases to 1.276, providing evidence of the transformation of Ti^{4+} to Ti^{3+}.

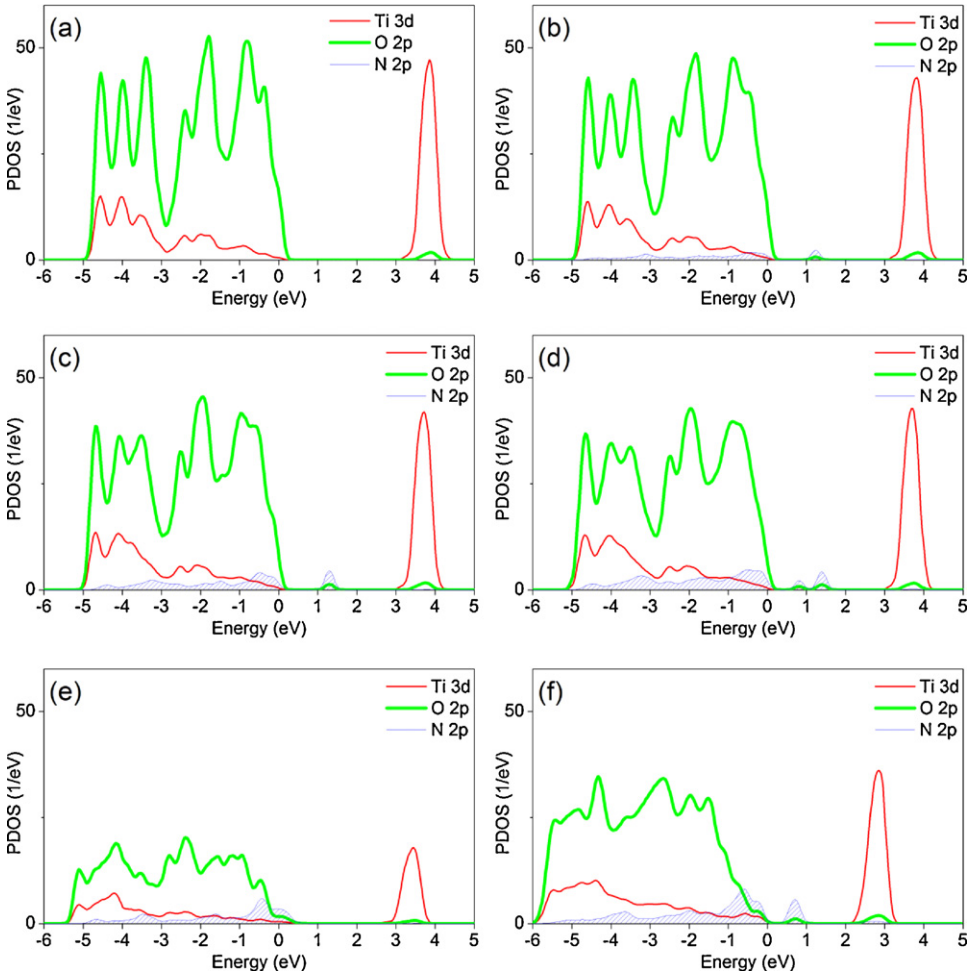

Fig. 6. The projected density of states (PDOS) of $TiO_{2-x}N_x$ with (a) $x = 0$, (b) $x = 0.0625$, (c) $x = 0.125$, (d) $x = 0.1875$, (e) $x = 0.25$ and (f) $x = 0.3125$.

4. Conclusions

Using the DFT + U method, this study investigated the influence of dopant concentration on the crystal structure, impurity formation energy, and electronic properties of N-doped anatase TiO_2. An effective Hubbard U of 8.47 eV was adopted to correctly determine the band gap. The calculated results show that under visible light, the mechanisms of photocatalytic activity are different for light nitrogen doping concentrations than for heavy concentrations. With light nitrogen doping, the mechanisms are the result of N isolated impurity states; however, with heavy nitrogen doping, the mechanisms are the result of a narrowing of the band gap and broadening of the valence band. These theoretical results provide insight into a number of controversial experimental observations.

Acknowledgements

This work was supported by the National Science Council in Taiwan (NSC 99-2221-E-131-023), for which the authors are grateful. We also acknowledge the National Center for High-performance Computing for computer time and the use of its facilities.

References

[1] J. Zhang, Y. Wu, M. Xing, S.A.K. Leghari, S. Sajjad, Energy Environ. Sci. 3 (2010) 715–726.
[2] R. Asahi, T. Morikawa, T. Ohwaki, K. Aoki, Y. Taga, Science 293 (2001) 269–271.
[3] Y. Nakano, T. Morikawa, T. Ohwaki, Y. Taga, Appl. Phys. Lett. 86 (2005) 132104–132106.
[4] H. Irie, Y. Watanabe, K. Hashimoto, J. Phys. Chem. B 107 (2003) 5483–5486.
[5] K. Yang, Y. Dai, B. Huang, J. Phys. Chem. C 111 (2007) 12086–12090.
[6] P.G. Wu, C.H. Ma, J.K. Shang, Appl. Phys. A 81 (2005) 1411–1417.
[7] X. Jiang, Y. Wang, C. Pan, J. Am. Ceram. Soc. (2011) 1–6.
[8] J. Ananpattarachai, P. Kajitvichyanukul, S. Seraphind, J. Hazard. Mater. 168 (2009) 253–261.
[9] J. Yu, S. Liu, Z. Xiu, W. Yu, G. Feng, J. Alloys Compd. 471 (2009) L23–L25.
[10] J. Zheng, Z. Liu, X. Liu, X. Yan, D. Li, W. Chu, J. Alloys Compd. 509 (2011) 3771–3776.
[11] M.V. Dozzi, S. Livraghi, E. Giamello, E. Selli, Photochem. Photobiol. Sci. 10 (2011) 343–349.
[12] H. Gao, C. Ding, D. Dai, J. Mol. Struct.: THEOCHEM. 944 (2010) 156–162.
[13] Y. Lv, L. Yu, H. Huang, H. Liu, Y. Feng, J. Alloys Compd. 488 (2009) 314–319.
[14] M.D. Segall, P.J. Lindan, M.J. Probert, C.J. Pickard, P.J. Hasnip, S.J. Clark, M.C. Payne, J. Phys.: Condens. Matter 220 (2002) 2717–2744.
[15] D. Vanderbilt, Phys. Rev. B 41 (1990) 7892–7895.
[16] H.J. Monkhorst, J.D. Pack, Phys. Rev. B 13 (1976) 5188–5192.
[17] S.L. Dudarev, G.A. Botton, S.Y. Savrasov, C.J. Humphreys, A.P. Sutton, Phys. Rev. B 57 (1998) 1505–1509.
[18] G. Shao, J. Phys. Chem. C 113 (2009) 6800–6808.
[19] R. Asahi, Y. Taga, W. Mannstadt, A.J. Freeman, Phys. Rev. B 61 (2000) 7459–7465.
[20] Z. Zhao, Q. Liu, J. Phys. D: Appl. Phys. 41 (2008) 025105.
[21] R. Long, N.J. English, J. Phys. Chem. C 114 (2010) 11984–11990.
[22] C.H. Ma, X.G. Ma, C.G. Li, L. Miao, J. Atom. Mol. Sci. 1 (2010) 78–86.
[23] J. Wang, D.N. Tafen, J.P. Lewis, Z. Hong, A. Manivannan, M. Zhi, M. Li, N. Wu, J. Am. Chem. Soc. 131 (2009) 12290–12297.